Radial Gradients in the Interplanetary Magnetic Field between 1.0 and 4.3 AU: Pioneer 10

by

Edward J. Smith
Jet Propulsion Laboratory
California Institute of Technology
Pasadena, California 91103

ABSTRACT

Radial gradients in the steady interplanetary field have been investigated between 1.0 and 4.3 AU using Pioneer 10 vector helium magnetometer data. The radial and azimuthal field components, the field magnitude and the spiral angle have been analyzed as functions of heliocentric distance. These four parameters were chosen because they could be compared directly with Parker's solar wind theory. It has been found that, in general, the observations agree with theory. The radial and azimuthal components appear to be reasonably well-described by the theoretically anticipated radial power law dependences. The field magnitude, although not following a simple power law, also agrees substantially with theory. At large distances the field continued to exhibit a definite spiral structure including well-defined magnetic sectors. The agreement between the observed spiral angle and the Parker spiral certainly appears adequate to first order, although there are significant second order deviations whose origin is unexplained at present. There is no substantial evidence for effects on the solar wind that might be attributed to its interaction with incoming interstellar gas. Radial gradients in the interplanetary field fluctuations between 1.0 and 4.3 AU have also been investigated using daily and hourly variances of the magnitude and three components. Although it may be possible to express the changes with distance as a simple power low, a better correlation exists between the variances and the square of the field magnitude. For both daily and hourly variances, the fluctuations are reasonably isotropic, with roughly equal power in all three components, and there is approximately an order of magnitude more power in the directional changes than in the fluctuations in magnitude. These results imply that, relative to the average field magnitude, the interplanetary field is as irregular at 4 AU as it is at 1 AU.

I. INTRODUCTION

The original theoretical model of the solar wind (Parker, 1958) predicted how the steady components of the interplanetary magnetic field would change with heliocentric distance. The theory assumed axial symmetry and dealt only with the radial and azimuthal field components parallel to the solar equatorial plane. The relation between these two components is given by the spiral angle, i.e., the angle between the interplanetary field and the radial direction. The theory is simplified in that longitudinal and time variations, which are responsible for sector structure, interacting fast and slow solar wind streams, etc. are ignored. More recent models have included both longitudinal and latitudinal asymmetries (Siscoe and Finley, 1970; Winge and Coleman, 1972; Suess and Nerney, 1973.) The simple Parker model has been used recently to predict the properties of the interplanetary field and the solar wind at large distances from the sun, principally in an attempt to examine the interaction of the heliosphere with the interstellar medium (Axford, 1972; Holzer, 1973).

It is important to compare recent observations of the interplanetary field in the outer solar system with Parker's theory. Such comparison provides an opportunity either to improve our physical understanding of the unimpeded expansion of the solar wind or to identify effects attributable to body forces exerted on the solar wind by incoming interstellar gas. If the former condition applies, it should be possible to determine the extent to which present theory is either adequate or requires modification. In any case, an understanding of how the magnetized solar wind changes as it flows outward from the sun is a prerequisite to identifying unambiguously such effects as may eventually be attributed to an interaction with the interstellar medium.

Previous attempts to test Parker's theory over radial distances from 0.7 to 1.5 AU have led to only marginal agreement. A study of the Mariner 4 data

acquired between Earth and Mars by Coleman et al. (1969) showed only partial agreement of the radial dependences of the field components with theory, while the spiral angle was found to be relatively unchanging. Measurements obtained between 0.8 and 1 AU by Pioneer 6 seemed qualitatively consistent with theory (Burlaga and Ness, 1968). However, subsequent analysis of Mariner 5 data obtained between 0.7 and 1.0 AU revealed significant discrepancies, including a tendency for the spiral angle to remain constant (Rosenberg and Coleman, 1973; Rosenberg, 1970). These puzzling results have led to several suggestions that attempt to modify Parker's theory in significant ways (Schatten, 1972; Rosenberg, 1970).

This report presents new observations obtained recently by Pioneer 10 over radial distances between 1.0 and 4.3 AU. The radial dependences of the radial and azimuthal field components and the field magnitude have been studied, as have the more subtle changes occurring in the spiral angle. This investigation has the advantage of covering a large range of heliocentric distances, but is subject to the same limitations as the earlier studies in that all are based on observations made by a single spacecraft. Thus, the spatial variations are confused by time variations associated with changing solar conditions, stream-stream interactions, etc. Eventually, it will be possible to compare directly simultaneous data from Pioneer 10 and Pioneer 11 at widely separated radial distances. However, only the observations made during the first year of the Pioneer 10 mission, prior to the Pioneer 11 launch, are reported here.

In addition to an analysis of the properties of the steady or average component of the interplanetary field, the behavior of the ever-present background fluctuations, which are associated with a multiplicity of physical causes, will be reported below. In a collisionless plasma, field fluctuations are the principal means by which energy is transferred from one form to another, whether as a result of stream-stream interactions or of basic plasma instabilities. In particular, the solar wind transport properties such as the thermal and electrical conductivities and viscosity are determined by the fluctuation spectrum. The long-period component of interplanetary field fluctuations is believed to cause scattering of primary cosmic rays at large heliocentric distances, thereby producing a spatial gradient in cosmic ray intensities as well as a modulation with solar activity. Parker (1963) has suggested that there will be a fundamental change in the nature of the fluctuations with increasing radial distance. As the spiral angle increases and the steady field gradually becomes predominantly tangential, he predicts a transition from a firehose to a mirror instability.

Variances in the three components and the field magnitude and their changes with radial distance have previously been studied by Coleman et al. (1969). The spectrum of the fluctuations near 1 AU is well-known from studies by Coleman, 1968; Siscoe et al., 1968; and Russell, 1972. The variances of the field components and the magnitude, determined from the Pioneer 10 data over daily and hourly intervals, and their changes between 1.0 and 4.3 AU will be presented below.

II. RADIAL GRADIENTS IN THE FIELD COMPONENTS, THE FIELD MAGNITUDE, AND THE SPIRAL ANGLE

For axisymmetric solar wind flow, which ignores effects of interacting fast and slow streams, the radial and azimuthal components of the interplanetary magnetic field are determined by two physical requirements (Parker, 1958). 1 The conservation of magnetic flux implies an inverse square dependence of the radial component:

$$B_R = B_R(1)/R^2 \quad ,$$

where $B_R(1)$ is the magnitude of the radial component at 1 AU and R is the heliocentric distance in AU. 2 The co-rotation electric field in the solar wind frame of reference, $(\vec{\Omega} \times \vec{R}) \times \vec{B}$, must be compensated by the convection field, so that the resultant vanishes. In the above expressions $\vec{\Omega}$ is the angular velocity of the sun and $\vec{V}$ is the velocity of the solar wind. This condition implies that

$$B_T = \frac{\Omega R}{V} B_R = \frac{\Omega}{V} \frac{B_R(1)}{R}$$

i.e., the tangential component, B_T, which is perpendicular to $\hat{R}$, parallel to the solar equatorial plane and positive in the direction of motion of the planets, decreases as R^{-1}. Alternatively, this condition specifies the spiral angle,

$$\psi = \text{Atan}\left(\frac{B_T}{B_R}\right) = \frac{\Omega R}{V} \quad .$$

The properties of the components and the field magnitude have previously been investigated over radial distances between 0.7 and 1.5 AU. Coleman et al. (1969), using data acquired by Mariner 4 between 1 and 1.5 AU while enroute to Mars, studied the radial dependences of the magnitudes of the radial and tangential components averaged over 27 days. Although both components decreased with distance, neither exhibited the expected power law dependences. A least squares fit yielded

$$B_R \propto R^{-1.23} \text{ and } B_T \propto R^{-1.22}$$

The combined result implied that the spiral angle was essentially independent of radial distance (see also Rosenberg, 1970).

Using Pioneer 6 data obtained between 1 and 0.8 AU, Burlaga and Ness (1968) had previously compared 29 day averages of B_R, B_T, and B with Parker's theory and demonstrated a qualitative agreement. At the previous Solar Wind Conference, Schatten (1972), confronted with these apparently contradictory results, proposed that variations in the solar wind velocity might lead to a violation of Parker's theory by 1 AU. However, an analysis of the Mariner 5 data obtained between Earth and Venus carried out by Rosenberg (1970) and Rosenberg and Coleman (1973) led to results similar to those obtained with Mariner 4. In this instance the best fit radial dependences were $B_R \propto R^{-1.78}$ and $B_T \propto R^{-1.85}$ again significantly different from theoretical expectations. Rosenberg (1970) noted a systematic difference between deviations from the Parker spiral during quiet and disturbed solar periods which he suggested were the effect of hydromagnetic waves and shocks.

Several factors make it difficult to study radial gradients using observations from a single spacecraft. The theory outlined above ignores azimuthal and temporal variations; however, as is well known, both assumptions are invalid. Very large longitudinal variations are present in the form of solar wind streams, the number and character of which undergo significant time changes between successive solar rotations. The strength and direction of the interplanetary magnetic field undergoes corresponding changes with longitude and time. During any given portion of the eleven year solar cycle, the latter may well be as large, or larger than, the theoretically expected changes with radial distance.

One of the advantages of the Pioneer 10 magnetic field investigation is the range of heliocentric distance covered (1 to 5 AU), far greater than for

previous missions. Thus the changes in the field are much larger, being a factor of 25 for the radial component and 5 for the tangential component. Even over this extended range, however, the spiral angle changes only from 45 to 79 degrees. The Pioneer investigation has the additional advantage that the measurements have been acquired over long periods of time (many solar rotations) and nearly continuously without significant data gaps. The necessity of accurately measuring fields an order of magnitude smaller than at 1 AU imposed stringent sensitivity and accuracy requirements on the magnetometer to be used. Fortunately, recent improvements in the vector helium magnetometer flown on Pioneers 10 and 11 have made it possible to measure such weak fields with relative ease. A description of the instrument, including its sensitivity and accuracy, is included here as an appendix.

A portion of the Pioneer data used in this study is shown in Fig. 1. The magnitudes of the three field components averaged over 24 hours are plotted as a function of time for the first 120 days of the mission. The corresponding radial distances are shown at the top of the figure and cover the range from 1.0 to 1.9 AU. The ever-present, very large temporal variations are an obvious feature of the data. In addition, another aspect of using averages of the magnitudes of the components causes further difficulties in trying to derive radial gradients.

There is a well-documented tendency for the interplanetary field to be organized into magnetic sectors in which the field points alternately toward and away from the sun (Davis et al., 1966, Wilcox and Ness, 1965). The average of any of the field components determined over intervals of approximately one solar rotation approaches zero. Hence, there is no steady "signal" whose radial dependence can be studied. To a first approximation the field is better characterized as a square wave alternating between positive and negative values at intervals of random duration.

It has been customary in past studies to determine the magnitude of a field component over relatively short intervals, much less than one day, and then to average these magnitudes over much larger intervals, comparable to a solar rotation. This procedure is equivalent to rectifying the signal to convert the irregular square wave into a DC signal. Unfortunately, all the irregularities superposed on these square waves are also rectified and the signal power which they represent then contributes to the steady signal. Subsequent averaging over longer time intervals is simply equivalent to low pass filtering the data, but this does not eliminate the power contributed at low frequencies by waves and other irregularities. Since the interplanetary field is well known to be highly irregular in direction, a significant amount of power is contributed by fluctuations whose own radial dependence may be different than those anticipated for the amplitude of the square wave signals.

To avoid these difficulties, a different approach has been adopted in this analysis based on the most probable value (the mode) of the field components (see Fig. 2). The data were organized into successive intervals of one solar rotation or 360^{o} of solar longitude as seen at Pioneer. This is equivalent to removing the co-rotation delay associated with the secular motion of Pioneer in the reference frame rotating with the sun. Three hour averages of the field components within each solar rotation were used to prepare amplitude probability distributions or histograms. The most probable value (MPV) or mode was then determined.

Initially, the histograms were two-sided (i.e., negative as well as positive values of the parameter and of the mode were studied). These were analyzed separately and compared with an analysis based on one-sided histograms, i.e., amplitude probability distributions of the magnitude of the field component. Either approach is free of the shortcomings associated with studying averages

of the absolute magnitudes of the components. The difference is principally a matter of the statistical uncertainties associated with the determination of the mode. Our preliminary analysis of both one-sided and two-sided histograms yielded essentially the same results and because of the convenience of handling a reduced amount of data, only the one-sided results will be presented below.

The statistical uncertainty associated with the most probable value was treated as follows. Several histograms were prepared based on the same data but using analysis intervals of different sizes. The mode was determined from the histogram corresponding to the smallest-sized interval that gave a clearly unambiquous primary peak. The analysis interval for that histogram was then used as a measure of statistical uncertainty associated with the mode. This procedure undoubtedly leads to an estimate of the uncertainty that is conservative in the sense that it is too large. However, it is justified in this instance because time variations from one solar rotation to the next were found to make a larger contribution to the residuals than uncertainties associated with determining the mode.

Histograms of three hour averages of the three components obtained at average radial distances of 1.04 and 4.3 AU are shown in Fig. 3a, b. Near 1 AU, the distributions for B_R and B_T have well defined peaks at $3 \pm 1\gamma$ and $2 \pm 1\gamma$ respectively, while the most probable value of B_N, the normal component which is orthogonal to $\hat{R}$ and $\hat{T}$ and positive northward, is zero within $\pm 1\gamma$. At 4.3 AU, according to the Parker model, the spiral angle is large and most of the field should be directed along $\hat{T}$. There is, indeed, a strong peak in B_T at $0.275 \pm .025\gamma$. The most probable value of B_R appears to be zero, a feature which might be associated with fluctuations, although there is a suggestion of a peak near 0.2γ, which is approximately the value expected at 4.3 AU for a 5 gamma field at 1 AU. Since the most probable value lies between 0γ and 0.2γ, a value of 0.1γ with a relatively large statistical uncertainty of $\pm 0.1\gamma$ was used in the analysis.

The most probable value of B_R, denoted $\hat{B}_R$, over successive solar rotations is shown as a function of heliocentric distance in Fig. 4 which is a log-log plot. The vertical lines represent the maximum and minimum values within which the peak in the histograms was found. The open circles are drawn at the midpoint of the interval. The straight line added for reference, corresponding to

$$B_R = 2.0/R^2 \quad ,$$

is seen to pass reasonably well through the data. There are only a few relatively large deviations, e.g., the value at 2.5 AU, which presumably can be attributed to time variations.

The most probable value of the tangential component, $\hat{B}_T$, is presented in a similar format in Fig. 5. In this case the line corresponding to $B_T = 1.5/R$ passes through the data reasonably well although the scatter is somewhat larger than in Fig. 3. A straight line corresponding to $B_T = 2.0/R$ would also fit the data with the principal exception of the three low values near 4 AU.

An alternative presentation of the data appears in Fig. 6. The most probable values of B_R multiplied by R^2 and of B_T multiplied by R are shown as linear functions of R. A dependence of R^{-2} and R^{-1} for B_R and B_T, respectively, should lead to the absence of any trend with increasing distance. Since there is no evidence of a trend in Fig. 5, reasonable agreement with Parker's model is indicated. The data obtained between 3 and 4.3 AU yield low values for B_R as well as B_T, suggesting that the magnitude of the field may have been low during this corresponding time interval.

The same techniques have also been applied to the normal component, B_N, to obtain preliminary information regarding this small component. In contrast, there is no evidence in the preliminary results that B_N obeys any well-behaved

radial dependence. The values decrease as the field gets smaller but appear to do so in a random way.

The radial dependences of B_R and B_T, since they agree with theory, imply that the direction of the field lies along the Parker spiral. However, as an alternative test of the theory, the most probable value of three hour averages of the spiral angle in the RT plane, i.e., ATAN $\left(B_T/B_R\right)$ has been studied as a function of radial distance. The approach used was essentially the same as that applied to B_R and B_T. The most probable value and the associated uncertainty were determined for successive 27 day solar rotations. Sample histograms of ψ obtained near 1.04 and 4.3 AU are shown in Fig. 7. The organization of the field into toward and away sectors is immediately evident in both and the spiral directions are quite well defined. Their most probable values agree well with the predictions of the Parker model. The arrows corresponding to theoretical values of ψ based on assuming $\tan \psi = R$, i.e. $\psi = 45^{\circ}$ at 1 AU.

Fig. 8 contains the most probable values of the spiral angle, $\hat{\psi}$, plotted as a function of heliocentric distance. Spiral angles corresponding to inward and outward sectors are plotted separately. The solid lines are theoretical values of ψ assuming a solar wind speed of 360 kilometers per second. The anticipated variation in ψ is rather modest for a change in R by a factor of 5. As with the components, the scatter in the observed $\hat{\psi}$, presumably owing to time variations at the sun, exceeds both the uncertainties associated with the mode and the theoretical changes. Nevertheless, there is a general trend in the data corresponding to the theoretical dependence. On the other hand, it would be difficult to argue that there is conclusive evidence of a significant deviation of observation from theory.

Fig. 9 contains the mode of the field magnitude (three hour averages) plotted as a function of radial distance. A theoretical curve, computed from

$$\left(B_R^2 + B_T^2\right)^{1/2} = B(1)\left(R^{-4} + R^{-2}\right)^{1/2}$$

and normalized to pass through as many of the data as possible is also shown. The curve fits the data between 1.5 and 3.0 AU very well for a normalization constant of $B(1) = 5\gamma$ (which implies an MPV of 7γ at 1 AU). The largest departures are at the ends of the distance range, the observations being high at 1.04 AU and low at 3.8 and 4.3 AU. The latter is consistent with other indications in Figs. 4 5, and 6 that the field magnitude decreased when Pioneer was near 4 AU, presumably as a consequence of a temporal change. Overall, the agreement between theory and observation is quite satisfactory.

III. RADIAL GRADIENTS OF THE FIELD FLUCTUATIONS: DAILY AND HOURLY VARIANCES

This preliminary study of the changes in the level of interplanetary fluctuations with radial distance is based on variances of the field magnitude and the three components. The variances represent the total power in the field irregularities associated with sources of all kinds: waves, discontinuities, stream-stream interactions, etc. One of the most effective means to distinguish between the various sources is to resolve the variances into components at different frequencies by computing power spectra. Since phase relations are often critical in distinguishing sources, it is advisable to compute cross spectra of the field components as well as auto spectra. In lieu of power spectral density calculations of the interplanetary fluctuations detected by Pioneer 10, which are being computed but which are not yet available, variances computed over two different intervals of one hour and twenty-four hours will be analyzed. At 1 AU, cross spectra have indicated a change in the character of the fluctuations at periods of a few hours (Goldstein and Siscoe, 1972). Fluctuations with characteristic periods of a few hours are apparently dominated by waves and discontinuities, whereas fluctuations with periods of 24 hours and longer seem to be dominated by effects associated with interacting solar wind streams. While many of the details cannot be investigated by simply studying variances, the gross behavior of the fluctuations should become apparent, such as whether or not the interplanetary field is becoming more or less irregular with increasing distance.

The Mariner 4 study by Coleman et al. (1969) included an investigation of the radial dependences of the field fluctuations over the range from 1.0 to 1.5 AU. The variances of the R, T, and N components over 3-hour and 24-hour intervals were found to have essentially the same radial dependence: $R^{-2.4 \pm 0.2}$. (The results were actually obtained for the standard deviations which have been converted to variances here simply by squaring the numbers in Coleman's article.) The variances in the field magnitude showed a dependence of the form: $R^{-1.4 \pm 0.2}$. The combined results imply that fluctuations in magnitude grow progressively more important with distance and that they become equal to the power in the steady field slightly beyond 4 AU.

The approach used here to study the variances parallels that adopted above to study the large scale or steady properties of the field. Variances of field parameter B_i, were computed in the usual way: $\sigma^2(B_i) = \langle B_i^2 \rangle - \langle B_i \rangle^2$, i.e., the mean of the square minus the square of the mean. Variances over 24 hours were calculated directly. Variances over successive one-hour intervals were accumulated to derive a daily average of the 1-hour variances. The variances were then grouped into longer intervals (27 days) corresponding to 360^0 of solar rotation as seen by Pioneer 10 (equivalent to removing the co-rotation delay between Pioneer and Earth). Histograms were prepared for each solar rotation and the most probable values were determined. The statistical uncertainties associated with the MPV's were obtained in essentially the same way as described above, i.e., they were taken to be one analysis interval ($\Delta\sigma^2$).

Typical time dependent behavior of $\sigma_D^2(B_R)$, the 24 hour or daily variances of B_R, at 1.04 and 4.3 AU is shown in Fig. 10. At 1 AU the power varies in an irregular manner between 1 and 10 γ^2 during one solar rotation. The variation is even larger at 4 AU, values between 10^{-2} and $1\gamma^2$ being recorded. The greater variability at large distances for this, the radial component, may arise because the field is nearly azimuthal making B_R sensitive to transverse fluctuations.

Fig. 11 contains the histograms for $\sigma_D^2(B_R)$ corresponding to Fig. 10. Near 1 AU, the MPV is $6.5 \pm 0.3\ \gamma^2$. A dramatic reduction in the level of the fluctuations is evident near 4 AU. The MPV lies between 10^{-1} and $10^{-2}\ \gamma^2$. A peak value of $3 \times 10^{-2}\ \gamma^2$ implies a reduction compared to $\sigma_D^2(B_R)$ at 1 AU by a factor of 200.

The MPV of the daily variances of B_R and B are shown in Fig. 12 as a function of radial distance. The vertical bars denote the analysis intervals within which the modes were found. The intervals for both B_R and B near 1 AU compare favorably with values of 5 and 1.4 γ^2 derived by Coleman et al. (1969). Neither set of data lies along a single straight line in this log-log plot. This deviation from a simple radial dependence may be attributed to time variations associated with the sun, as were the departures from Parker's theory in the section above. The straight lines having an R^{-4} dependence pass through both sets of data better than either R^{-3} or R^{-5}. The separation between the two lines implies a relatively constant ratio of 6 between $\hat{\sigma}_D^2(B_R)$ and $\hat{\sigma}_D^2(B)$.

This figure also contains the square of the MPV of the field magnitude $\hat{B}^2$, the data previously presented in Fig. 9 above. It is evident that the variations in $\hat{\sigma}_D^2(B_R)$ and $\hat{\sigma}_D^2(B)$ track the variations in $\hat{B}^2$ very well, certainly much more closely than they follow a simple radial dependence. The overlap between corresponding intervals (vertical lines) for $\hat{\sigma}_D^2(B_R)$ and $\hat{B}^2$ can be maximized by taking $\hat{\sigma}_D^2(B_R) \approx 0.2\ \hat{B}^2$. If the same procedures are applied to the variance in B, the result is $\hat{\sigma}_D^2(B) \approx .03\ \hat{B}^2$. Again, the ratio of the variances in the radial component and in the total field is a factor of approximately 6.

The daily variances in the two transverse components, B_T and B_N, are shown as functions of radial distance in Fig. 13. As in Fig. 12, straight lines corresponding to $8R^{-4}$ and $\hat{B}^2$ are included for reference. The same conclusion is drawn: the variances in B_T and B_N are better correlated with $\hat{B}^2$ than with a radial dependence. It can readily be seen that both variances agree closely with $0.2\ \hat{B}^2$. This is consistent with a direct comparison of Figs. 12 and 13 which shows that the power in each of the three field components is essentially the same and approximately six times larger than the power in the magnitude fluctuations. The proportionality constant between the variances and $\hat{B}^2$ is determined in this way to within better than a factor of two.

Figs. 14 and 15 contain the corresponding data for the hourly variances. A good correlation of the four variances with $\hat{B}^2$ is again evident. The maximum overlap between the statistical uncertainties in the variances and in $\hat{B}^2$ occurs for

$$\hat{\sigma}_H^2(B_R) \approx \hat{\sigma}_H^2(B_T) \approx .05\ \hat{B}^2,\ \hat{\sigma}_H^2(B_N) \approx 0.1\ \hat{B}^2$$

and

$$\hat{\sigma}_H^2(B) \sim .01\ \hat{B}^2.$$

The proportionality constants are again known to within better than a factor of two.

These results imply that the variances in the components are again approximately equal, although $\hat{\sigma}_H^2(B_N)$ may be slightly larger than for the other two components by a factor of two. The power in each component is 5 to 10 times larger than the power in the magnitude variations, just as for the daily variances. Finally, the power at high frequencies is less than that at low frequencies as anticipated. A comparison of the daily and hourly variances shows the former to be larger by factors of 3 ± 1.

IV. CONCLUSIONS AND DISCUSSION

A. The Steady Field: Components, Magnitude and Spiral Angle

Radial gradients in the steady interplanetary magnetic field have been investigated between 1.0 and 4.3 AU using Pioneer 10 vector helium magnetometer data. The radial and azimuthal field components, the field magnitude and the spiral angle have been analyzed as functions of heliocentric distance. To avoid potential difficulties associated with averaging the magnitudes of the components, the analysis was based on the most probable values (the modes) of B_R and B_T obtained from histograms of three-hour averages of each component accumulated over 360^o of solar longitude (one solar rotation). It was also expected that the ratio of the modes of B_R and B_T would not correctly yield the spiral angle, since, in general, the mode of the joint probability distribution of two variables is not simply related to the modes obtained from the probability distributions of the individual variables. Therefore, the spiral angle was computed directly from the field measurements and three-hour averages were used to derive amplitude probability distributions of ψ over successive solar rotations. The MPV of ψ was then found and analyzed as a function of radial distance. The same approach was applied to the field magnitude. These four parameters were chosen because they could be compared directly with theory (Parker, 1958). The north-south or normal component, B_N, was de-emphasized in this study because its existence is not predicted by simple solar wind theory and because it is typically much smaller than the other parameters and hence more difficult to determine accurately. Thus, the investigation of this important aspect of the interplanetary field is deferred to some future study.

It has been found that, in general, the observations agree with theory. The radial and azimuthal components appear to be reasonably well-described by $\hat{B}_R \approx 2/R^2$ and $\hat{B}_T \approx 1.5/R$ (Figs. 4 and 5), both of which match the theoretically anticipated radial power law dependences. The field magnitude, although not following a simple power law, also agrees substantially with theory (Fig. 9). There are significant departures of individual data points from the foregoing relations which are attributed to temporal variations of the interplanetary field parameters from one solar rotation to another.

At large distances, the field continued to exhibit a definite spiral structure, including well-defined magnetic sectors (Fig. 7). The average values and maximum deviations of the observed spiral angles for toward (negative) and away (positive) sectors (Fig. 8) were:

$$\hat{\psi}(-) = 62^o \pm \frac{28}{32} \quad \text{and} \quad \hat{\psi}(+) = 67^o \pm \frac{33}{17} .$$

In comparison with the theoretical values corresponding to reasonable solar wind velocities, which lead to $\psi = 67^o \pm \frac{12}{16}$, the agreement with the Parker spiral certainly appears adequate to first order. The overall agreement is particularly impressive when one considers the full range of values from 0 to 360^o that are potentially available to ψ (Fig. 8).

There are, however, significant deviations of individual values of $\hat{\psi}$ from the theory, departures of up to 30^o being observed. In a few cases, $\hat{\psi}$ exceeded 90^o, a result that is qualitatively inconsistent with the simple theory which relates the field direction to the co-rotation electric field. These second order discrepancies do not appear to be explainable as the consequence of long-period variations in the solar wind speed or of variations in the solar wind speed or direction at interaction fronts between slow and fast streams. The observed maxima and minima average values for the solar wind speed cannot account for deviations of 20 or 30^o on the basis of $\text{Tan}\ \psi = \Omega R/V$ and fast-slow deflections are typically less than 10^o.

There are several important conclusions based on the overall agreement between observation and theory. Contrary to the earlier studies using Mariner

data, it has been found that the Pioneer data are consistent with the anticipated radial dependences. The Pioneer data also show that the spiral angle tends to increase with radial distance as anticipated, although there is some disordering of ψ whose origin is unexplained at present. These differences may be associated with the earlier studies having been based on averages of the magnitudes of the components, a procedure equivalent to rectification. The Pioneer investigation has the additional important advantage of covering a much greater range of heliocentric distances. Both the Mariner and Pioneer studies showed that the magnitude of the field behaves as theoretically expected.

There is no substantial evidence for effects on the solar wind that might be attributed to its interaction with incoming interstellar gas. If such effects are present, they are apparently being obscured by the relatively large ever-present time variations and a more careful and subtle analysis will be required to detect them. It seems at least as plausible that, out to 4 or 5 AU, the solar wind is expanding at a relatively unimpeded way, except for the internal effect of fast stream-slow stream interactions.

B. Field Fluctuations: Daily and Hourly Variances

Radial gradients in the interplanetary field fluctuations between 1.0 and 4.3 AU have been investigated using daily and hourly variances of the magnitude and three components. The actual parameters that were analyzed were the most probable values of the variances obtained from histograms composed of data acquired over 360° of solar longitude or one solar rotation (Fig. 11). Although it may be possible to express the changes with distance (Figs. 12 through 15) as a simple power law, a better correlation exists between the variances and the square of the field magnitude (actually the mode of the latter determined over one solar rotation). The daily variances of the radial, tangential, and normal components and of the field magnitude obeyed the following approximate relations: $\hat{\sigma}_D^2(B_R) \approx \hat{\sigma}_D^2(B_T) \approx \hat{\sigma}_D^2(B_N) \approx 0.2\ \hat{B}^2$ and $\hat{\sigma}_D^2(B) \approx .03\ \hat{B}^2$.

The corresponding relations for the hourly variances are: $\hat{\sigma}_H^2(B_R) \approx \hat{\sigma}_H^2(B_T) \approx .05\ \hat{B}^2$, $\hat{\sigma}_H^2(B_N) \approx 0.1\ \hat{B}^2$ and $\hat{\sigma}_H^2(B) \approx .01\ \hat{B}^2$. Thus, for both daily and hourly variances, the fluctuations are reasonably isotropic, with roughly equal power in all three components, and there is approximately an order of magnitude more power in the directional changes than in the fluctuations in magnitude.

Although a power law of the radial distance is a convenient functional dependence to investigate, there is no obvious reason why the field fluctuations should obey such a relation. Although the radial and azimuthal components follow a power law, other parameters that may be important to the relevant physics involved, such as B or B^2, do not obey a simple power law. The R^{-4} fits shown above (Figs. 12, 13) are probably accidental. They are based principally on the data at the beginning and end of the interval, i.e., at 1 and 4 AU. However, there is some evidence in the behavior of the steady fields that a major time variation caused $\hat{B}$ to decrease while Pioneer 10 was near 4 AU and this could have caused an apparent spatial variation. When all the data are considered, the correlation with $\hat{B}^2$ is clearly better.

The proportionality between the energies in the fluctuations and in the steady field implies σ/B is also approximately constant with distance. This means the field is just as irregular at 4 AU as it is at 1 AU. Since this invariance applies specifically to the ratio, $\hat{\sigma}_D^2(B)/\hat{B}^2$, the inference of Coleman, et al. (1969) that the level of fluctuations in magnitude would approach the average field by 4.3 AU is contrary to the Pioneer results.

It is not at all obvious why the relation $\sigma^2/B^2 \approx$ constant should hold. It is possible that there is approximate equi-partition between forms of internal energy so that the wave energy density, $\sigma^2/8\pi$ is correlated with the thermal energy density, nkT.

If, in addition, $\beta = 8\pi nkT/B^2$ should tend to be constant in the solar wind, perhaps with a value near 1 as observed near 1 AU, the level of the fluctuations would then correlate with variations in B as observed.

The ratio of the daily to hourly variances depends on the shape of the underlying power spectral density of the field fluctuations. For time stationary signals, the variance is simply the integral over frequency of the power spectral density. If the spectrum follows a power law of the form f^{-n}, an additional few simplifying assumptions make it possible to derive an approximate expression for the exponent, n, based on the ratio of the variances:

$$n - 1 \approx \log (\sigma_D^2/\sigma_H^2)/\log 24$$

Thus, the observed ratio of 3 ± 1 implies a spectral shape of the form $f^{-1.3 \pm 0.1}$. This inference is reasonably consistent with the spectra between frequencies of 1 cpd and 1 cph computed by Coleman, et al. (1969) near 1 AU. This may imply that between 1 and 4 AU the spectrum is relatively unchanging over the frequency range investigated in this study.

V. APPENDIX

Since experience with the vector helium magnetometer (VHM) is limited to our own research activities, this appendix provides background information regarding the instrument and the particular features of the Pioneer 10 investigations that are relevant to the study of radial gradients of the interplanetary field. The Pioneer VHM is an advanced version of an instrument flown to Mars and Venus on Mariners 4 and 5 (Slocum and Reilly, 1963, and Connor, 1968). A more complete description of the Pioneer investigation is also available (Smith, 1973).

The basic mode of operation of the magnetometer is as follows. The essential sensor elements consist of a helium lamp, a circular polarizer, a helium absorption cell, Helmholtz coils, a lens, and an infrared detector. The basic operation of the magnetometer depends upon the effect of the magnetic field direction on the efficiency with which metastable helium can be optically pumped. The presence of an ambient magnetic field causes a sine wave modulation of the infrared radiation passing through the gas cell at the fundamental frequency of an applied circular sweep field. The magnetometer output voltage is developed across a precision resistor in series with a nulling coil used to generate a field which cancels the ambient field.

The primary instrument requirements on a mission to the outer solar system are sufficient sensitivity to detect field variations an order-of-magnitude smaller than the steady field, say .01γ or less, and sufficient stability to measure the steady field with the relative accuracy of better than 10%. The latter figure has been a typical achievement near 1 AU and this level of precision has generally proven adequate for most scientific studies.

One of the principle advantages of the VHM is its high level of sensitivity. The power spectral density of the inherent instrument noise, converted to an equivalent fluctuating field at the sensor, is independent of frequency (white

noise) with a value of $\simeq 10^{-4}\ \gamma^2/Hz$. Thus, extremely high sensitivity at frequencies below 1 Hz can be achieved by using a low pass filter. The operation of averaging the digitized, telemetered data after receipt at Earth is equivalent to digital, low pass filtering. Thus, averages over a few seconds reduce the pass band to below 1 Hz and the noise power spectral density is then equivalent to a background of $10^{-2}\ \gamma$ RMS. A demonstration of this high level of sensitivity is provided by Fig. 16 which contains one minute averages of the magnitude and the three components of the interplanetary field during a quiet interval of 3 hours while Pioneer 10 was at 4.3 AU. Another potential limitation to the sensitivity, the digitization noise associated with converting the analog wave forms into digital signals, has a power spectral density that is typically less than $10^{-4}\ \gamma^2/Hz$. Since the averages used in this study are much longer than a few seconds, there is essentially no instrument noise contribution to any of the results presented above.

The accuracy of analog magnetometers such as the VHM is determined principally by: (1) the scale factor, $k = \Delta B/\Delta V$, where V is the voltage corresponding to field component, B, and (2) the magnetometer offset, B_0, which conceptually represents the output in zero field. Since the VHM is a closed loop instrument, the relatively large amount of negative feedback assures that the BV relation is highly linear, in this case to within .01%. Thus, the calibration relation between the output, V, and the ambient field is simply

$$B = B_0 + kV$$

As a consequence, the accuracy depends only on how well B_0 and k are known in flight.

Pre-flight calibrations were conducted at regular intervals of several months in order to obtain a high accuracy and to accumulate evidence regarding stability. The scale factors were determined by applying accurately known ($\pm$1/2%) calibration fields to the sensor. The magnetometer offsets were determined in the standard manner which involves flipping the sensor by 180^0 to distinguish the offset from any ambient field that may be present.

The conventional approach to checking the magnetometer scale factors in flight is to apply calibration field changes, ΔB, to the sensors so that the corresponding ΔV can be determined. Normally several step changes are applied sequentially so that the linearity can be tested directly. The Pioneer in-flight-calibration, which was initiated by ground command every few weeks, used fields of ± 13 and $\pm 26\gamma$ to calibrate the low ranges on which the instrument operated in interplanetary space. After two years of in-flight-calibrations, no change has been detected in the Pioneer 10 scale factors which are then known to an accuracy of 1% or better.

The offsets were independently determined in flight using two different techniques. The two axes in the equatorial plane of Pioneer, which was spin stabilized, automatically rotated through 360^0 every $\simeq$ 12 seconds (the Pioneer spin period). Thus, the offsets on these two axes could be determined by simply averaging their outputs over a large number of complete rotations. The offset on the magnetometer axis parallel to the Pioneer spin axis was determined by an adaptation of the variance technique (Belcher, 1973) which was developed by L. Davis, Jr. for application to a spinning spacecraft. The essential assumption is made that over short intervals of time (5 minutes), the fluctuations in the interplanetary field are principally changes in direction and tend to conserve the magnitude of the field.

An error analysis of the above equation indicates that the maximum relative error is

$$\Delta B/B \lesssim \Delta B_0/B + \Delta k/k$$

$\Delta B/B \leq \Delta B_0/B + \Delta k/k$

A term representing the relative error contributed by the digitization uncertainty, which is negligible compared to the other two terms, has been deleted.

It has already been stated that $\Delta k/k \leq .01$. The most significant error is undoubtedly contributed by the uncertainties associated with the in flight determination of the offsets, particularly the component parallel to the spacecraft spin axis. A measure of the relative uncertainty associated with the latter was obtained as follows. Daily estimates of the offset obtained by the variance technique were used to compute standard deviations of the estimates over intervals of two weeks. The standard deviations were then divided by the average field magnitudes over the same intervals to derive an estimate of $\Delta B_0/B$. Over radial distances from 1.0 to 4.3 AU, the range covered in this report, the ratio of the standard deviation of the offset determinations to the field magnitude was consistently less than .05.

If this ratio is substituted into the above expression, the relative maximum error $\Delta B/B < .06$. Therefore in a 5γ field, corresponding for example to 1 AU, the absolute error is < 0.3γ. At larger distances, e.g. 4 AU where the average field is approximatly 1γ, $\Delta B < .06\gamma$. The use above of the standard deviation as a measure of the uncertainty is a conservative procedure. The probability that the actual offset exceeds the standard deviation is very small. It is customary in statistical inference to use the standard error, i.e., the standard deviation divided by the square root of the number of observations, which is approximately a factor of 3 smaller.

ACKNOWLEDGEMENTS

My co-investigators on the Pioneer 10 magnetic field investigation are: D. S. Colburn, P. J. Coleman, Jr., L. Davis, Jr., P. Dyal, D. E. Jones, and C. P. Sonett. This is a preliminary report of a study in progress that is being carried out in collaboration with R. Rosenberg and P. J. Coleman, Jr. The reduction of the large masses of Pioneer data implicit in this analysis was carried out by J. Hull, C. Stanley, L. Shaw, and L. Burrus of the JPL Ground Data Handling Group with the assistance of B. V. Connor. I was assisted in analyzing the data by B. Tsurutani and by E. Parker who did all the computer programming and made the production runs. Conversations with P. J. Coleman, Jr. and L. Davis, Jr. regarding the results were very helpful. This report represents one phase of work carried out by the Jet Propulsion Laboratory for the National Aeronautics and Space Administration under Contract No. NAS7-100.

REFERENCES

Axford, W. I., The Interaction of the Solar Wind with the Interstellar Medium, in Solar Wind, Ed. C. P. Sonett, P. J. Coleman, Jr., and J. M. Wilcox, NASA Sci. and Tech. Info. Office, Wash., p. 609 (1972).

Belcher, J., A Variation of The Davis-Smith Method for In-Flight Determination of Spacecraft Magnetic Fields, J. Geophys. Res. 78, 6480 (1973).

Burlaga, L. F. and N. F. Ness, Macro- and Micro-Structure of the Interplanetary Magnetic Fields, Can. J. Phys. 46, 5962 (1968).

Coleman, P. J., Jr., Turbulence, Viscosity, and Dissipation in the Solar Wind Plasma, Ap. J. 153, 371 (1968).

Coleman, P. J., Jr., E. J. Smith, L. Davis, Jr., and D. E. Jones, The Radial Dependence of the Interplanetary Magnetic Field: 1-1.5 AU, J. Geophys. Res. 74, 2826 (1969).

Connor, B. V., Space Magnetics: The Mariner V Magnetometer Experiment, IEEE Trans. on Magnetics, Vol. MAG-4, 391 (1968).

Davis, L., Jr., E. J. Smith, P. J. Coleman, Jr., and C. P. Sonett, Interplanetary Magnetic Measurements, The Solar Wind, JPL Tech. Report 32-630, Pasadena, p. 35 (1966).

Goldstein, B. and G. L. Siscoe, Spectra and Cross Spectra of Solar Wind Parameters from Mariner 5, in Solar Wind, Op. Cit., p. 506 (1972).

Holzer, T. E., Interaction of the Solar Wind with the Neutral Component of the Interstellar Gas, J. Geophys. Res. 77, 5407 (1972).

Parker, E. N., Dynamics of the Interplanetary Gas and Magnetic Fields, Ap. J. 128, 664 (1958).

Parker, E. N., Interplanetary Dynamical Processes, InterScience Publishers, New York, 154-159 (1963).

Rosenberg, R. L., Twenty Seven Day Deviations of the Interplanetary Magnetic Field and Plasmas from the Parker Spiral Model, J. Geophys. Res. 75, 5310 (1970).

Rosenberg, R. L. and P. J. Coleman, Jr., The Radial Dependence of the Interplanetary Magnetic Field: 1.0-0.7 AU, pub. no. 1196-26, Instit. of Geophys. and Planet. Phys., UCLA (1973).

Russell, C. T., Comments on the Measurement of Power Spectra of the Interplanetary Magnetic Field, in Solar Wind, Op. Cit., p. 365 (1972).

Schatten, K. H., Large Scale Properties of the Interplanetary Magnetic Field, in Solar Wind, Op. Cit., p. 65 (1972).

Siscoe, G. L. and L. T. Finley, Solar Wind Structure Determined by Corotating Coronal Inhomogeneities, J. Geophys. Res. 75, 1817 (1970).

Siscoe, G. L., L. Davis, Jr., P. J. Coleman, Jr., E. J. Smith, and D. E. Jones, Power Spectra and Discontinuities of the Interplanetary Magnetic Field: Mariner 4, J. Geophys. Res. 73, 61 (1968).

Slocum, R. E. and F. N. Reilly, Low Field Helium Magnetometer for Space Applications, IEEE Trans. on Nucl. Sci. NS-10, 165 (1963).

Smith, E. J., The Pioneer-Jupiter Magnetic Field Investigation, JPL Tech. Report 616-48 (1973).

Suess, S. T. and S. F. Nerney, Meridional Flow and the Validity of the Two-Dimensional Approximation in Stellar-Wind Modeling, Ap. J. 184, 17 (1973).

Wilcox, J. M. and N. F. Ness, Quasi-Stationary Corotating Structure in the Interplanetary Medium, J. Geophys. Res. 70, 5793 (1965).

Winge, C. R., Jr. and P. J. Coleman, Jr., Magnetic Latitude Effects in the Solar Wind, Solar Wind, Op. Cit., p. 609 (1972).

the data from Fig. 5 multiplied by R. Horizontal straight lines, $B_R R^2$ = 2.0 and $B_T R$ = 1.5 pass through the two sets of data reasonably well.

Fig. 7: Histograms of three hour averages of the spiral angle at 1.0 and 4.3 AU. The data in the upper and lower panels were acquired during one solar rotation while Pioneer was near 1 and 4 AU respectively. The spiral field structure and the presence of toward (quadrant II) and away (quadrant IV) sectors is evident. The vertical arrows at the bottom of each panel represent theoretical values computed from ψ = atan (R) i.e., $\Omega R/V = 1$ at 1 AU.

Fig. 8: Most probable values of the spiral angle as a function of radial distance. The vertical lines represent the histogram interval ($\pm 10^o$, compare Fig. 7) within which the mode has been found to lie. Sectors in which the field points toward the sun corresponds to ψ values located in the bottom half of the figure. The two curves were computed from ψ = ATAN (1.22R) which was then adjusted to correspond to toward and away sectors and to positive values of the angle being counter-clockwise as viewed from the north.

Fig. 9: The most probable values of three hour averages of field magnitude as a function of radial distance. The data format is essentially the same as in Figs. 4 and 5. The normalized curve passing through the data has the radial dependence predicted by Parker's theory.

Fig. 10: Daily variances of the radial fluctuations at 1 and 4 AU as a function of solar longitude. The data acquired on a given day were identified with a corresponding day of a solar rotation by taking into account the radial and corotation delays associated with the Pioneer trajectory. A nominal solar wind speed of 360 km/sec, the most probable value as measured at 1 AU, was assumed on making this first order correction. The data are plotted logarithmically with those obtained near 1 AU in the upper panel.

Fig. 11: Histograms of the daily variances of the radial fluctuations. The two histograms correspond to the variances shown in Fig. 10. Because of the large range in the values of the variances, a logarithmic histogram interval was used in these and all subsequent variance histograms.

Fig. 12: Daily variances in the radial component and in field magnitude and the square of the field magnitude as functions of radial distance. The vertical lines correspond to histogram intervals associated with three parameters (from bottom to top): The MPV of the daily variance in field magnitude, $\hat{\sigma}_D^2(B)$, the MPV of the daily variance in the radial component, $\hat{\sigma}_D^2(B_R)$, and (in grey tone) the square of the MPV of the field magnitude (given in Fig. 9), $\hat{B}^2$. Two straight lines are shown corresponding to $\sigma^2(B_R) = 8/R^4$ and $\sigma^2(B) = 1.5/R^4$.

Fig. 13: Daily variances of the tangential and normal components as functions of radial distance. Each panel also contains the square of the MPV of the field magnitude, $\hat{B}^2$, for reference (grey tone) and a straight line corresponding to $8/R^4$.

Fig. 14: Hourly variances of fluctuations in the radial components and in field magnitude. Again here, data corresponding to $\hat{B}^2$ (grey tone) have been included for reference.

Fig. 15: Hourly variances of fluctuations in the tangential and normal components. The same format is used as in Fig. 13.

Fig. 16: Magnetometer data sample of the quiet interplanetary field. One-minute averages of the magnitude and the three field components over a 3-hour interval are shown. Pioneer was at a radial distance of 4.0 AU and the field was only 0.5γ and was very quiet. The small variations which can be seen ($\sigma \simeq .05\gamma$ rms) are significantly larger than the instrument noise and are real fluctuations of the interplanetary field.

SIGNAL DETECTION USING PROBABILITY DISTRIBUTION

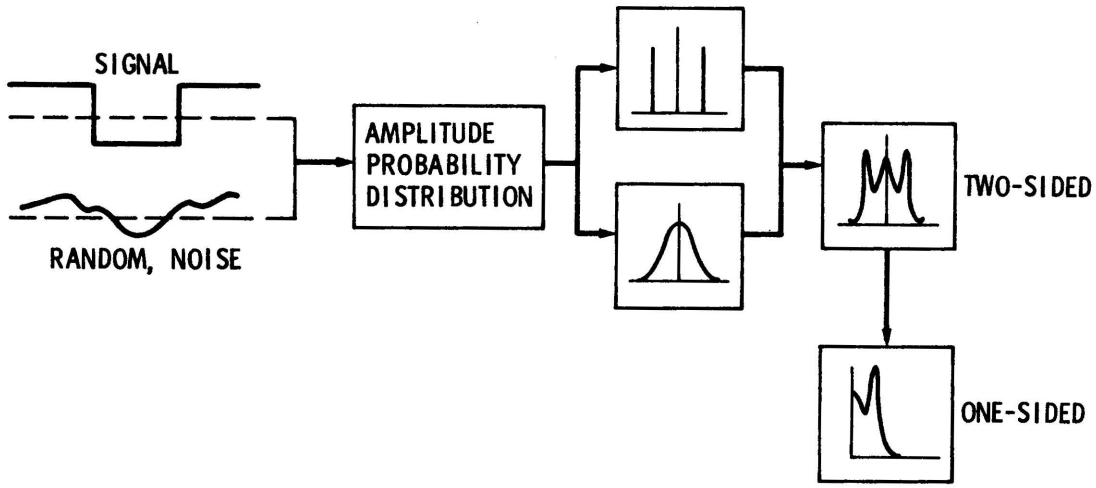

FIGURE 2

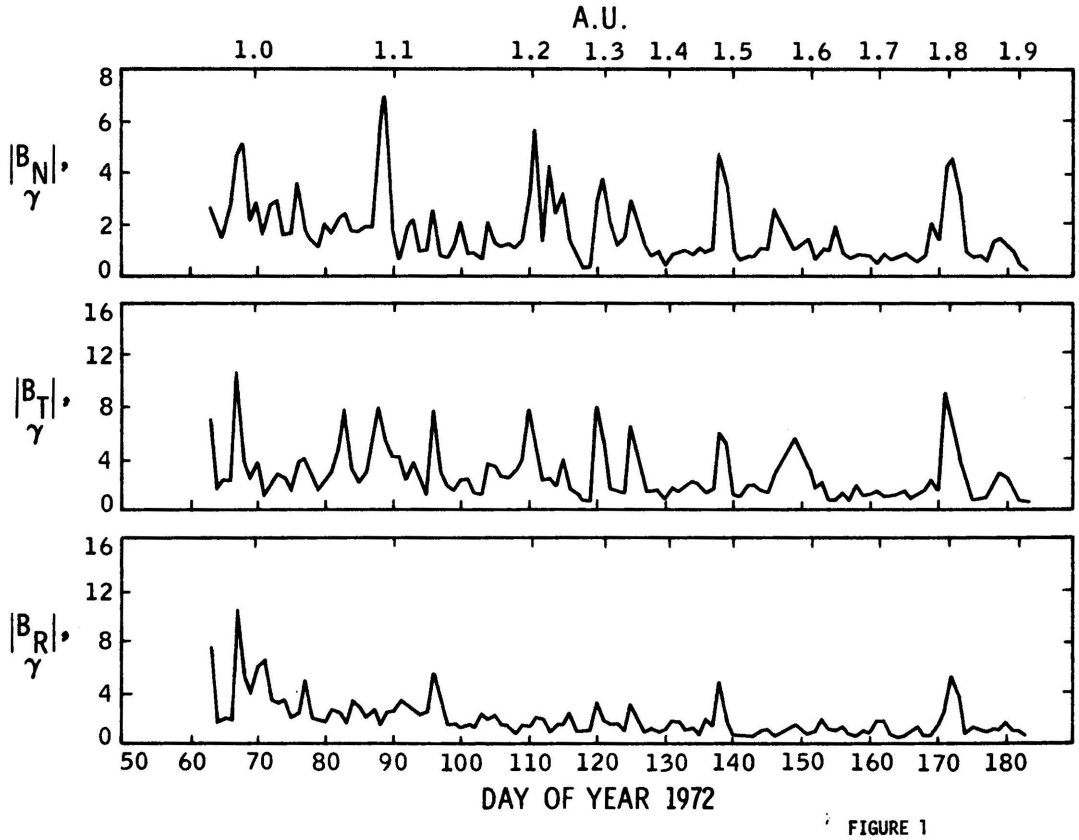

FIGURE 1

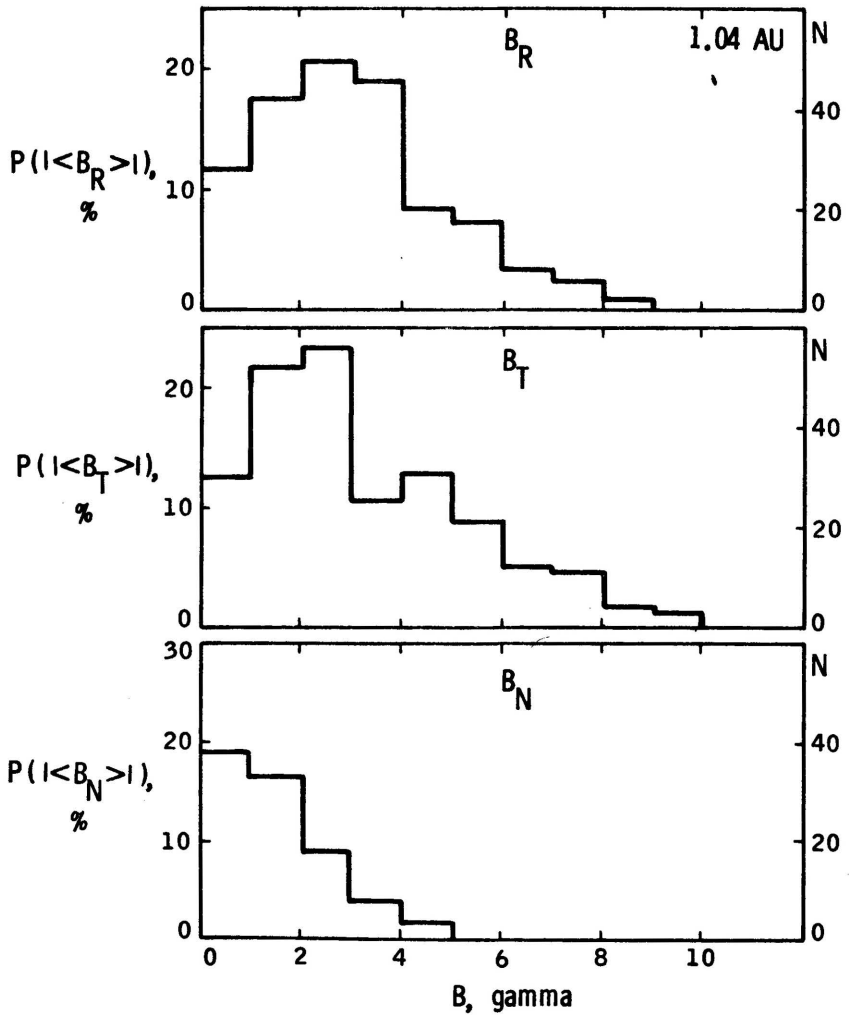

FIGURE 3a

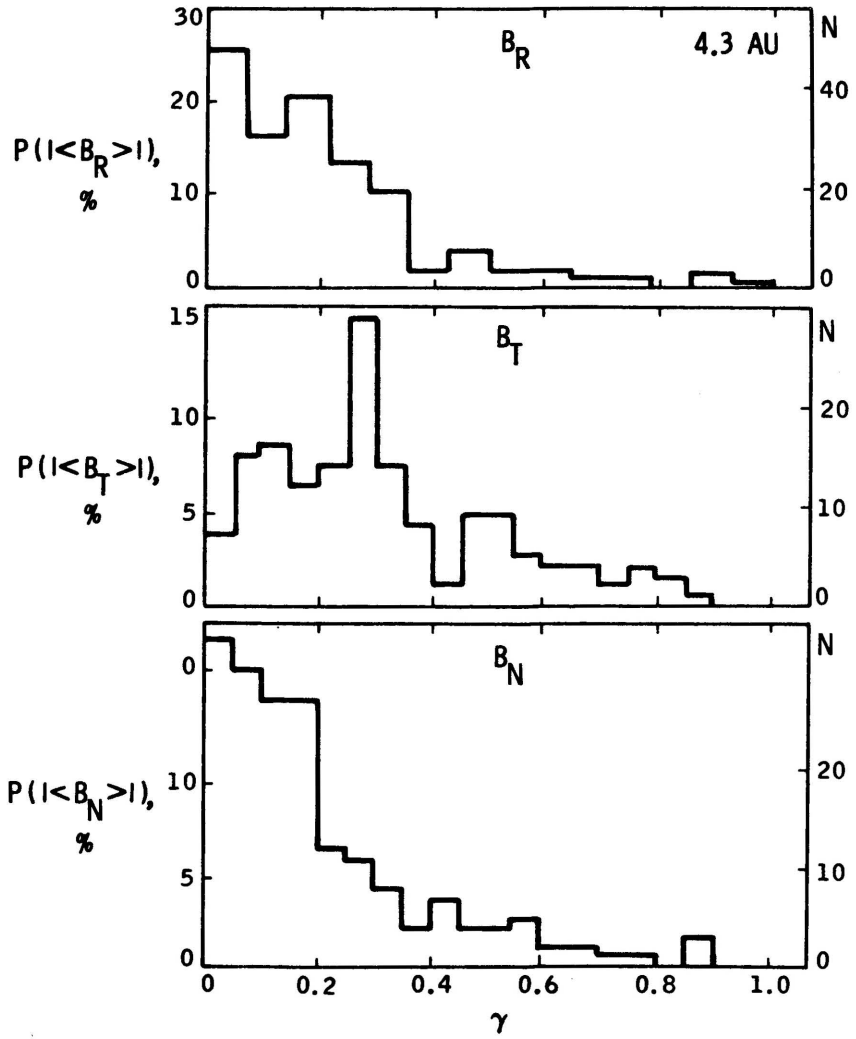

FIGURE 3b

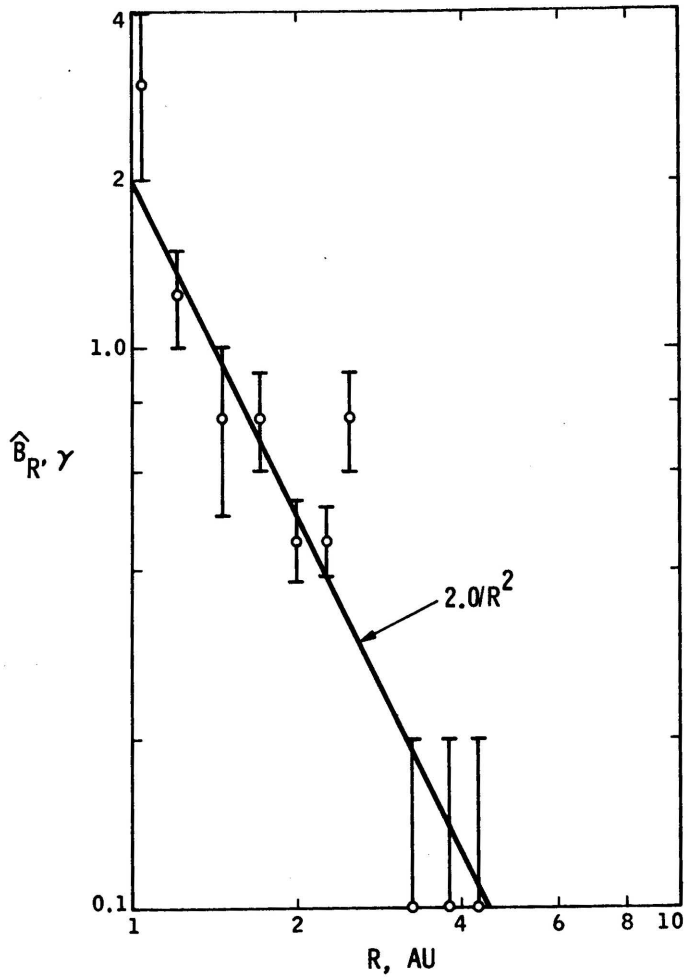

FIGURE 4

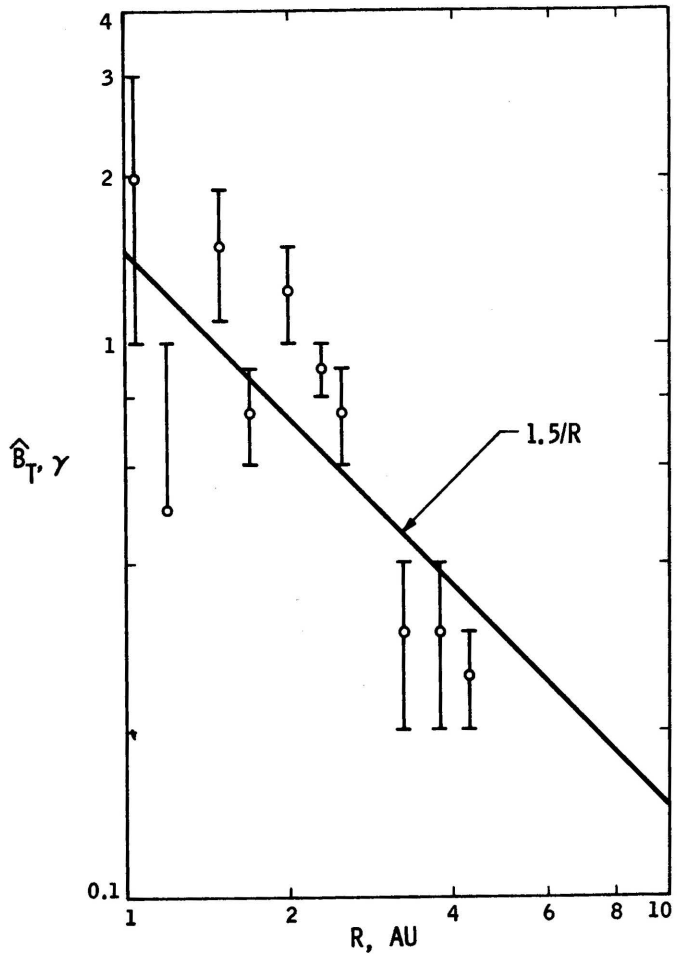

FIGURE 5

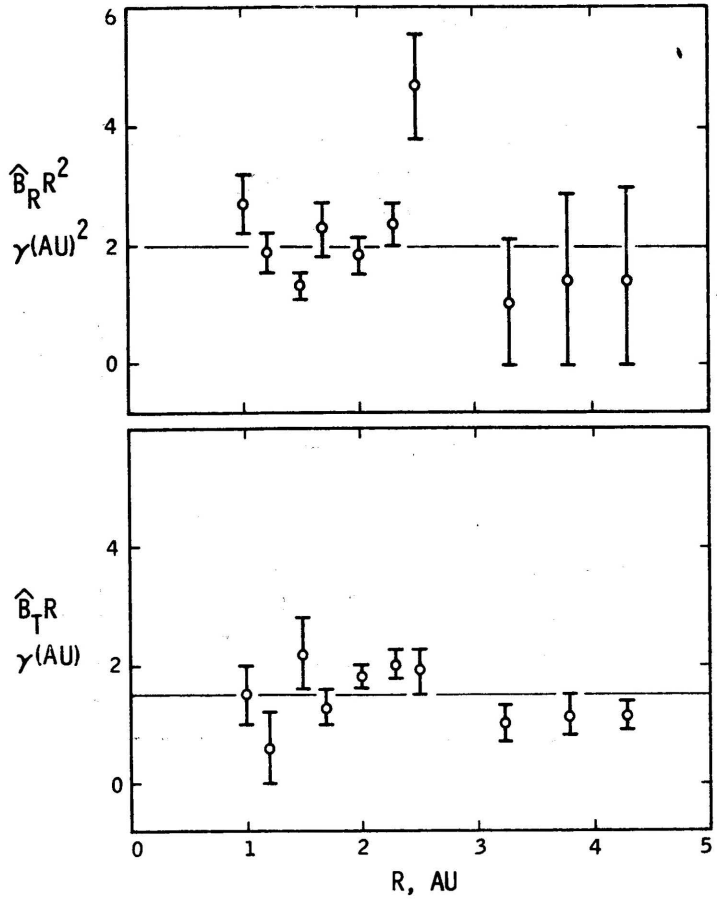

FIGURE 6

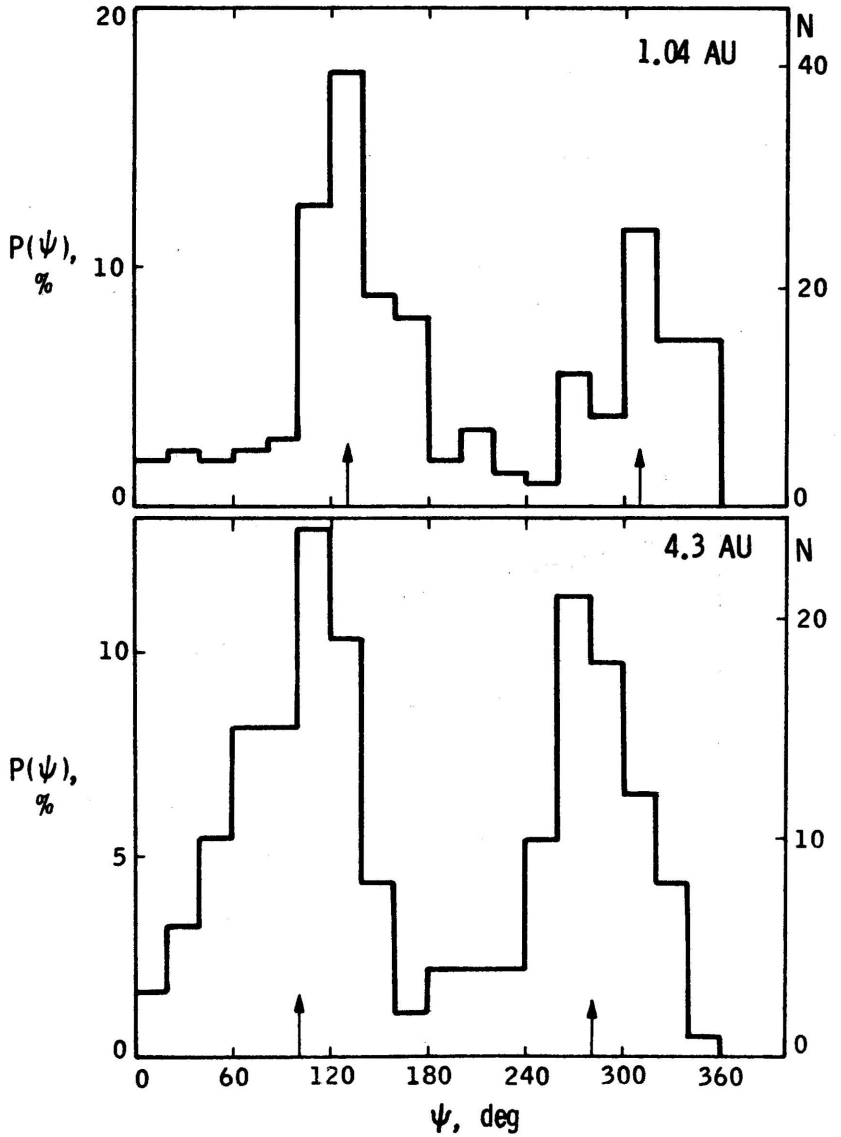

FIGURE 7

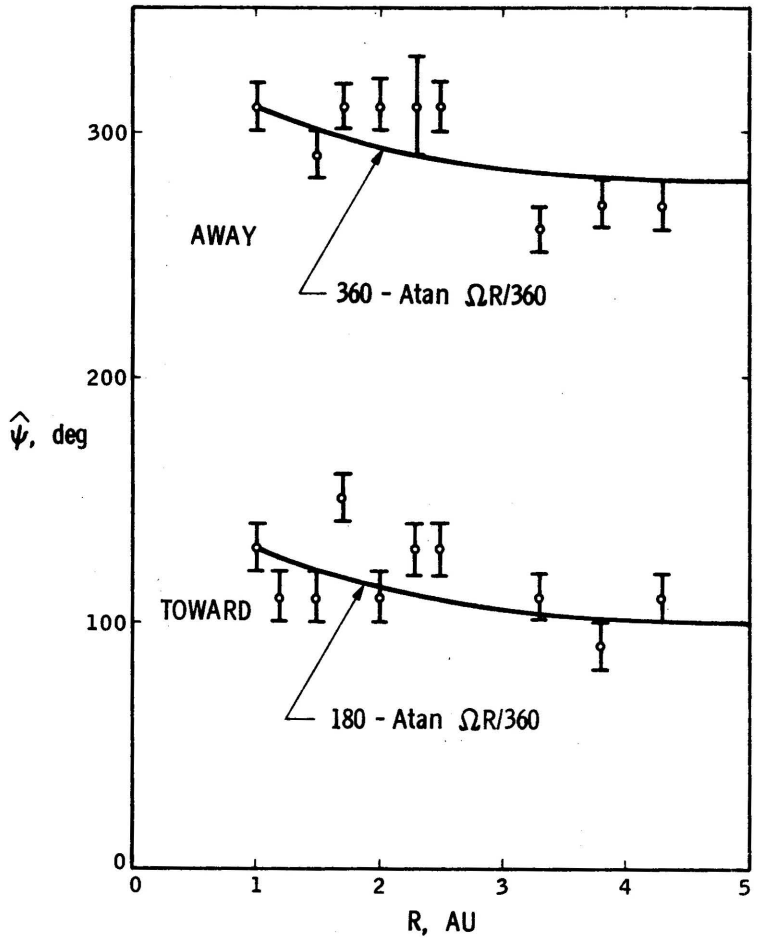

FIGURE 8

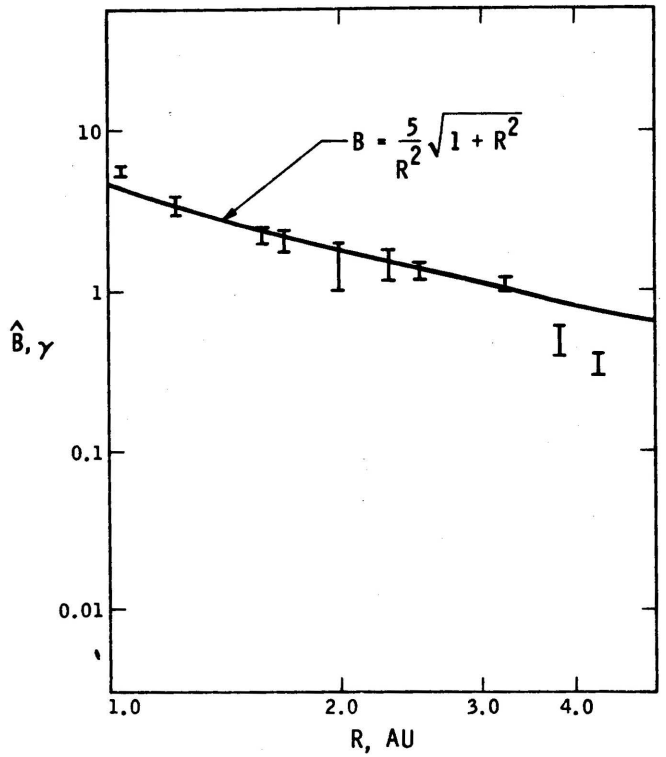

FIGURE 9

FIGURE 8

FIGURE 9

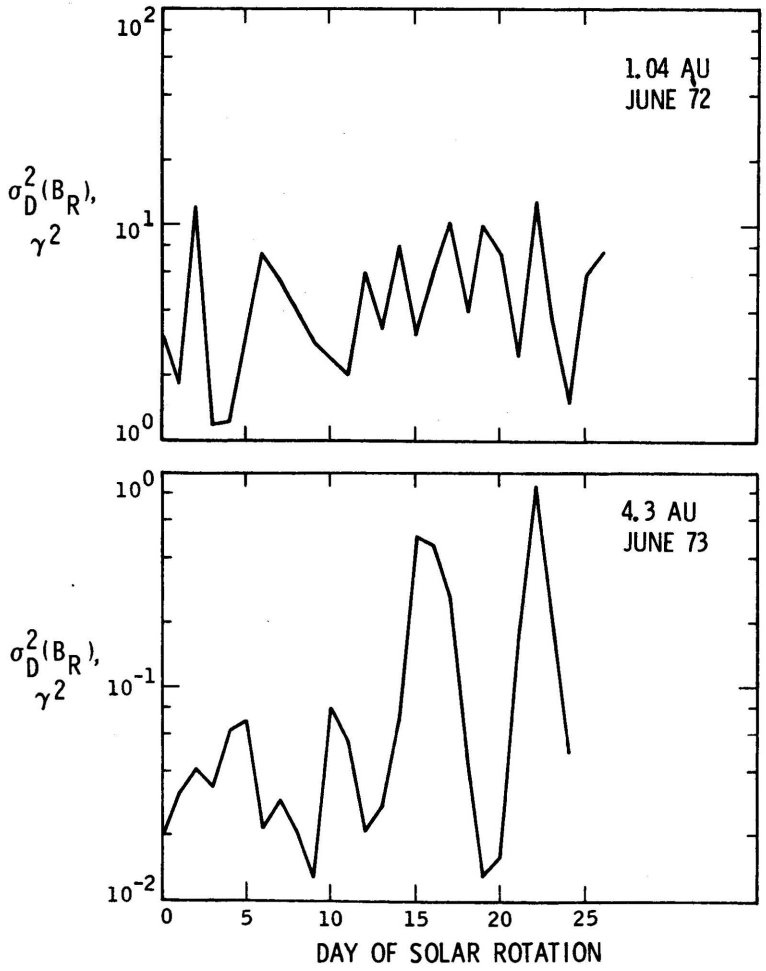

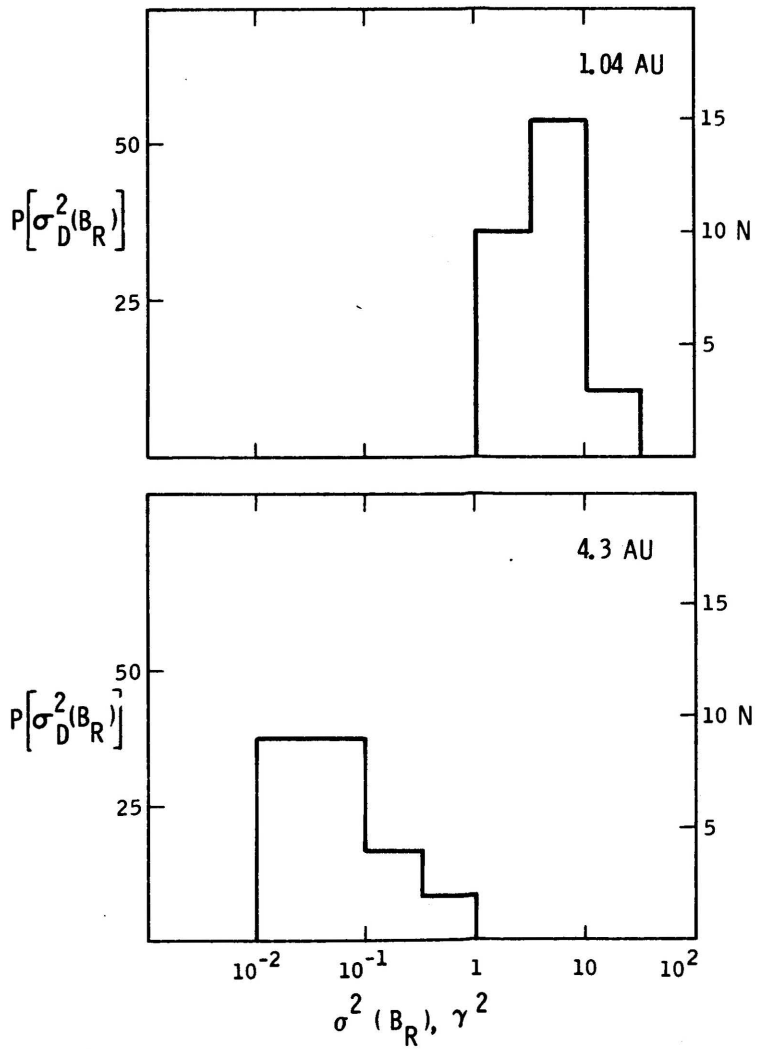

FIGURE 10

FIGURE 11

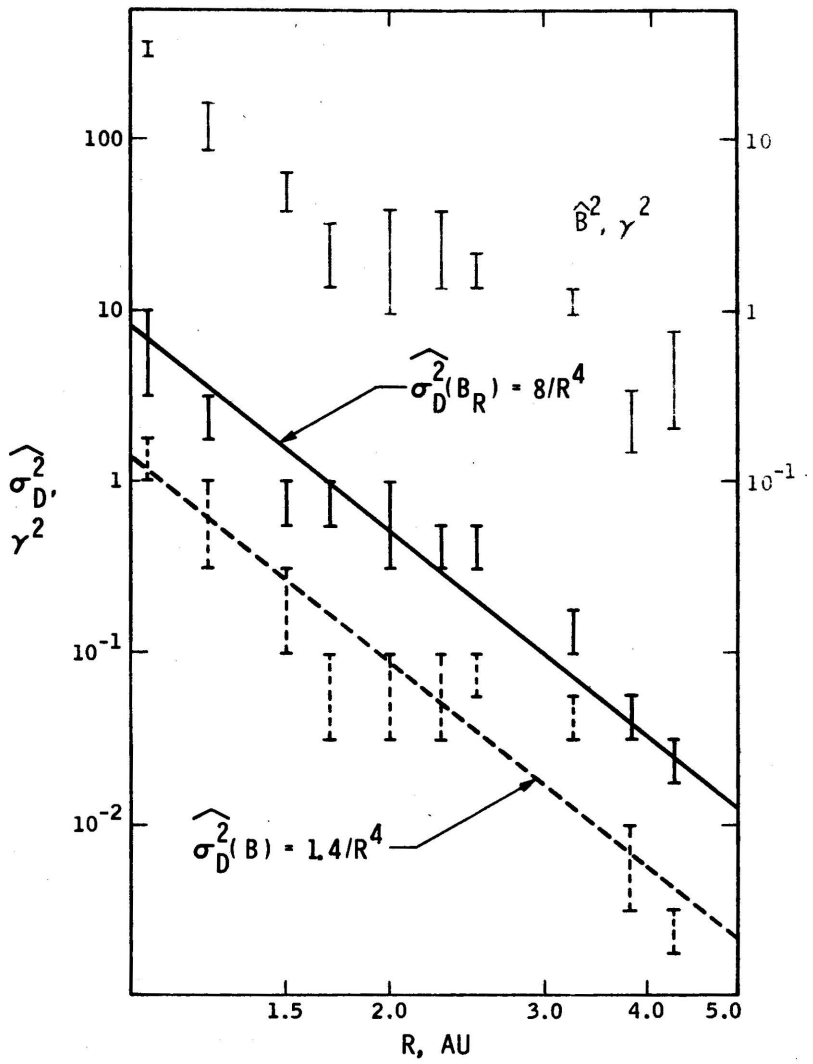

FIGURE 12

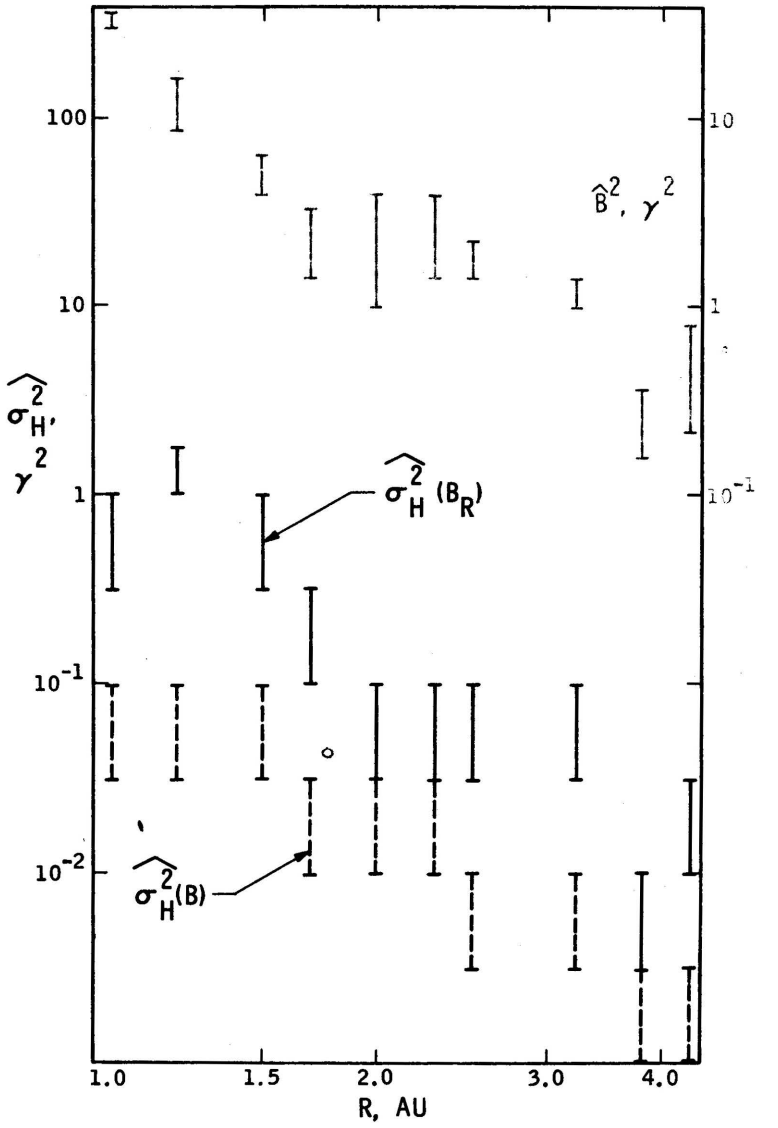

FIGURE 14

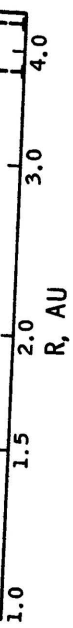

FIGURE 14

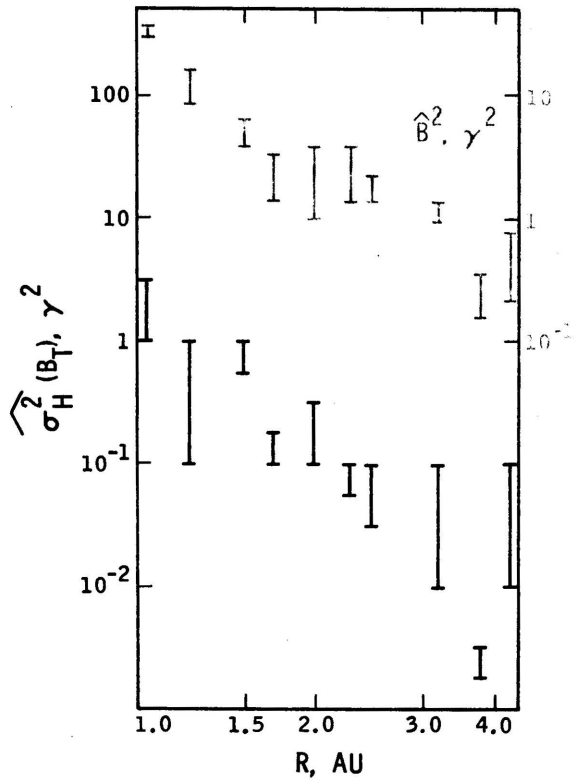

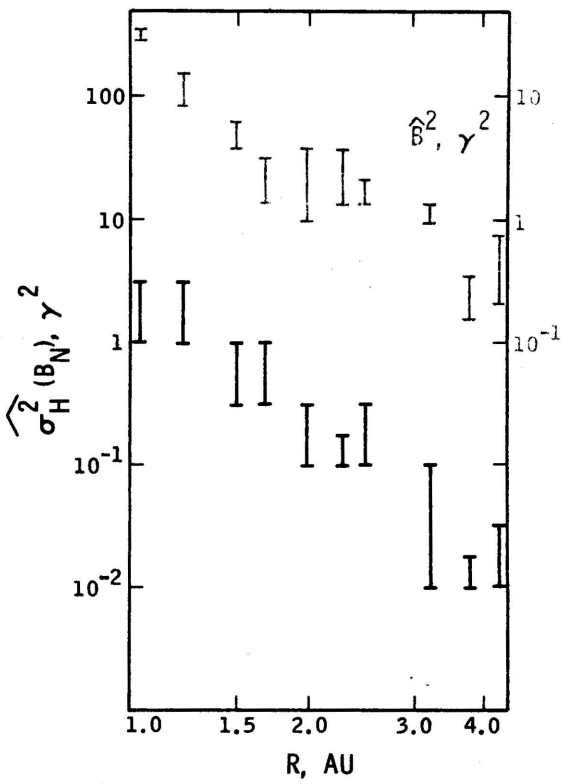

FIGURE 15

FIGURE 12

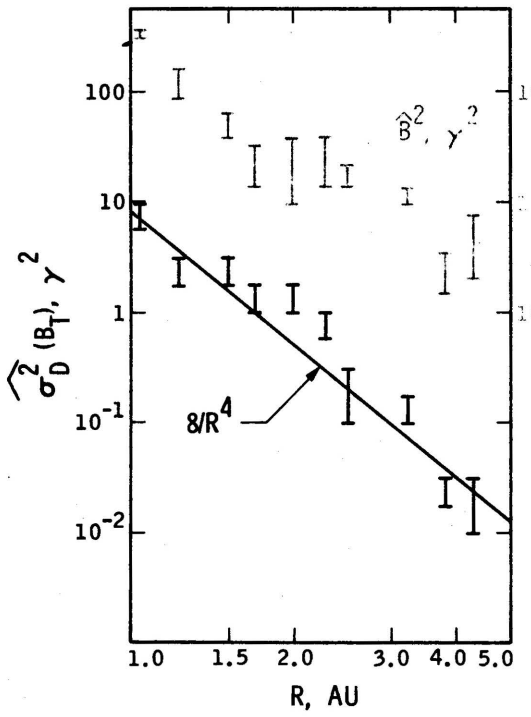

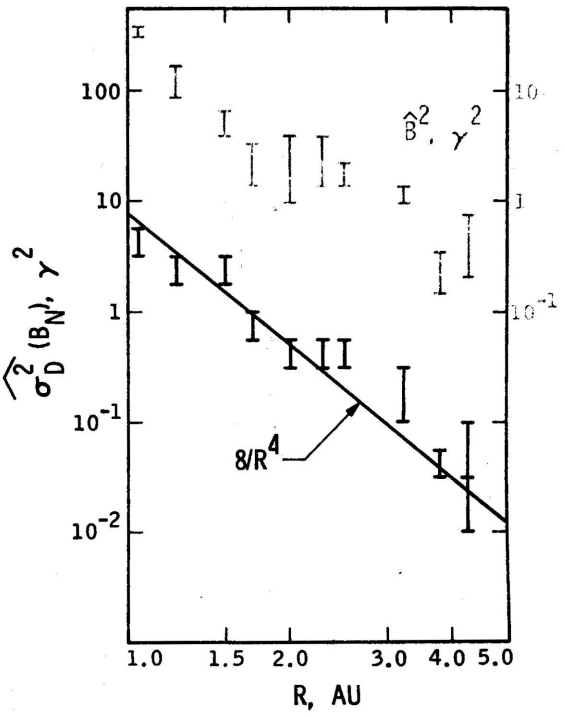

FIGURE 13

PIONEER 10 MAGNETOMETER
ONE MINUTE AVERAGES
16 APR 1973

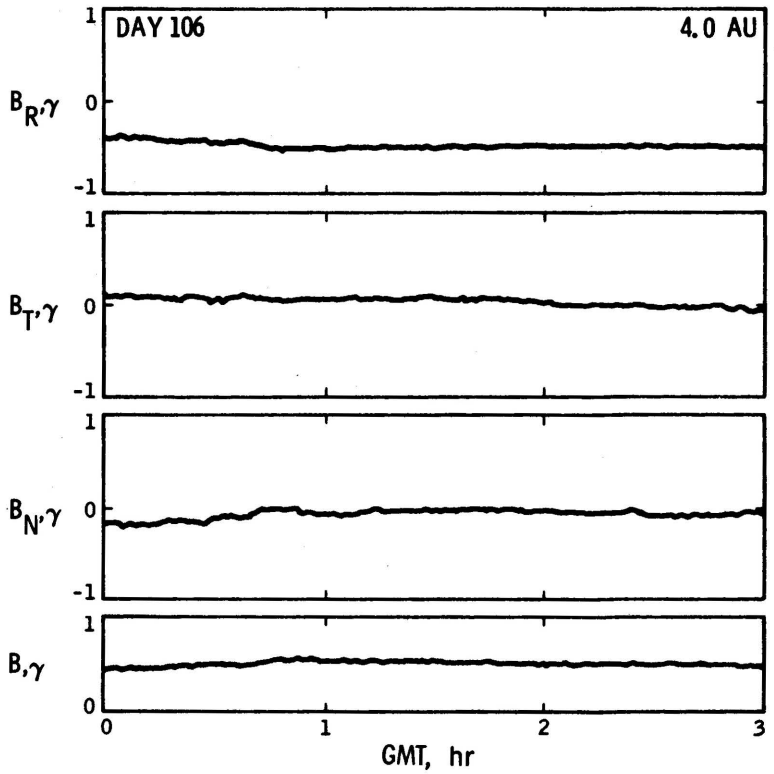

FIGURE 16